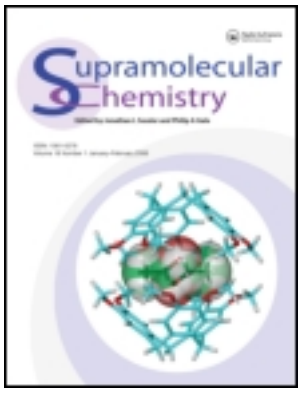

Supramolecular Chemistry
Publication details, including instructions for authors and subscription information:
http://www.tandfonline.com/loi/gsch20

Anion influenced self-assembly of stilbazolium derivative and acid-sensitive property of its corresponding gel

Jun Hou [a], Xue Wu [a] & Yuan-Jie Li [a]

[a] Key Laboratory of Natural Resources of Changbai Mountain & Functional Molecules, Yanbian University, Ministry of Education Yanji, Gongyuan Road 977#, Yanji City, Jilin Province, 133002, P.R. China

Available online: 03 May 2011

To cite this article: Jun Hou, Xue Wu & Yuan-Jie Li (2011): Anion influenced self-assembly of stilbazolium derivative and acid-sensitive property of its corresponding gel, Supramolecular Chemistry, 23:7, 533-538

To link to this article: http://dx.doi.org/10.1080/10610278.2011.563951

Supramolecular Chemistry
Vol. 23, No. 7, July 2011, 533–538

Taylor & Francis
Taylor & Francis Group

Anion influenced self-assembly of stilbazolium derivative and acid-sensitive property of its corresponding gel

Jun Hou, Xue Wu* and Yuan-Jie Li

Key Laboratory of Natural Resources of Changbai Mountain & Functional Molecules, Yanbian University, Ministry of Education Yanji, Gongyuan Road 977#, Yanji City, Jilin Province 133002, P.R. China

(*Received 18 November 2010; final version received 31 January 2011*)

Two stilbazolium derivatives with different counter-anions (Br^- and OH^-) have been designed and synthesised. Different counter-anions cause different aggregation properties. The reason of this difference was investigated through concentration- and temperature-dependent ^1H NMR and IR spectra. When the counter-anion is OH^-, the stilbazolium derivative exhibits pronounced aggregation properties. The scanning electron microscope images of xerogels show the characteristic gelation morphologies of 3D fibrous network structures. X-ray diffraction and fluorescence spectroscopy studies have been carried out, and provide more information to define the molecular packing model in gelation states. Finally, the acid-sensing abilities of the xerogel film were studied.

Keywords: gels; pyridinium; counter-anion; acid sensitivity

Introduction

Recently, low-molecular weight organogels (LMOGs) have attracted increasing interest because of their potential applications, such as sensors (*1–3*), drug delivery (*4*, *5*) and template synthesis (*6–9*). LMOGs are the materials in which the gelator self-assembled through non-covalent interactions to form 3D networks which can immobilise a large amount of solvents (*10–13*). Generally, the cooperative effect of non-covalent forces mainly includes hydrogen bonding, $\pi-\pi$ stacking, dipolar, electrostatic force and van der Waals interactions. Therefore, particular functional sites, such as H-bond-forming site, long alkyl chain and $\pi-\pi$ stacking unit, are necessary for the gelation (*10*, *12*). The $\pi-\pi$ interaction, which has generated both theoretical and experimental interest in recent years, is an important interaction for the construction of supermolecular architectures. Compared with $\pi-\pi$ interaction, cation$-\pi$ interaction has stronger interactive force (*14–16*). Some interesting host–guest complexes and supermolecular structures were constructed through this force (*17*, *18*). Of all kinds of organic cations, pyridinium cation always serves as the cationic parts of the cation$-\pi$ systems. Some gelators containing pyridinium moiety have been reported (*19*, *20*). However, there is no systematical study about the influence of counter-anion to the gelation.

The oligo(*p*-phenylenevinylene) (OPV) derivatives display outstanding supramolecular assembly properties (*21–24*) and their self-assemblies possess some specific utilities, such as energy transfer (*25*), photoluminescence switching (*26*), imaging (*27*) and white lighting emission devices (*28*), owing to their unique optoelectronic properties. In this contribution, we introduced pyridinium moieties into a conventional OPV unit to form a stilbazolium derivative with two different counter-anions (Br^-, **OPVBr**; OH^-, **OPVOH**). Considering that van der Waals interactions are helpful for organogel systems, two long *N*-alkyl chains were introduced. When the counter-anion is Br^-, the stilbazolium derivative did not exhibit satisfied gelation properties. Changing the counter-anion to OH^- could well improve the gelation ability of the stilbazolium derivative. On the basis of the $\pi-$cation interaction of stilbazolium core and hydrogen bonding between OH^-, OPVOH exhibited good thermoreversible gelation property in acetonitrile. Its corresponding gel was acid sensitive.

Result and discussion

The preparation procedure of **OPVBr** and **OPVOH** is outlined in Scheme 1. **OPVBr** was synthesised by a simple condensation reaction with a good yield (76%). The *trans* configuration was confirmed by the *J* value (16.4 Hz) of the vinylic protons in its ^1H NMR spectra. **OPVOH** was obtained by treating **OPVBr** with anion exchange resin. The change of counter-anion was confirmed by MALDI-TOF MS. Figure 1 shows the MS singles at *m/z* 912.83, 894.82 and 878.82, which corresponded to M^+, $[M - OH^-]^+$ and $[M - 2OH^-]^+$, respectively.

The gelation ability of **OPVBr** and **OPVOH** was tested by dissolving them in a variety of solvents with

*Corresponding author. Email: wuxue@ybu.edu.cn

ISSN 1061-0278 print/ISSN 1029-0478 online

DOI: 10.1080/10610278.2011.563951
http://www.informaworld.com

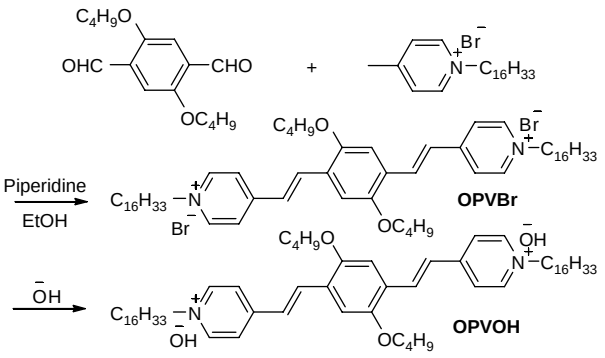

Scheme 1. The synthesis and structure of the stilbazolium derivatives.

gentle heating. After cooling down, if the solvent was apparently immobilised without fluid by inverting the vial, it was considered as gel. The results are given in Table 1. Interestingly, it was found that **OPVBr** could only gel in *n*-octanol at 4°C. In the case of **OPVOH**, gelation could occur in acetonitrile at room temperature and in nitrobenzene at 4°C. The critical gel concentration (CGC) of **OPVBr** in *n*-octanol was 35 mg ml^{-1}, whereas that of **OPVOH** in acetonitrile and nitrobenzene was 5 and 30 mg ml^{-1}, respectively. These phenomena indicate that different anions can make the assembly behaviour significantly different, and the nature of the solvents has considerable influence on the gelation behaviour of **OPVBr** and **OPVOH**.

In order to investigate the aggregation morphology of the organogel, the xerogel of **OPVBr** from *n*-octanol and **OPVOH** from acetonitrile was prepared and subjected to the scanning electron microscope (SEM) observation. As shown in Figure 2, the SEM image of **OPVBr** xerogel revealed a flocculent network. In the case of **OPVOH** xerogel, the image revealed a network structure composed of intertwined fibres with a width of 200–300 nm. It has been reported that the gelation of low-molecular weight molecules is a result of the gelator–gelator and solvent–gelator interactions, and the gelator molecules tend to assemble into bigger aggregates with higher gelator–gelator interactions (*29*). The reason for the flocculent network of OPVBr in *n*-octanol may be due to weak solvent–gelator interactions in this system.

The self-assembly mechanism of **OPVBr** and **OPVOH** was investigated by NMR, FT-IR, Fl and X-ray diffraction (XRD) spectroscopy. First, the concentration-dependent ^{1}H NMR of **OPVBr** and **OPVOH** in $CDCl_3$ at room temperature was recorded and is shown in Figures 3 and 4, respectively. Increasing the concentration of **OPVBr** resulted in a downfield shift of the aromatic protons and N–CH_2 proton signals. In the case of

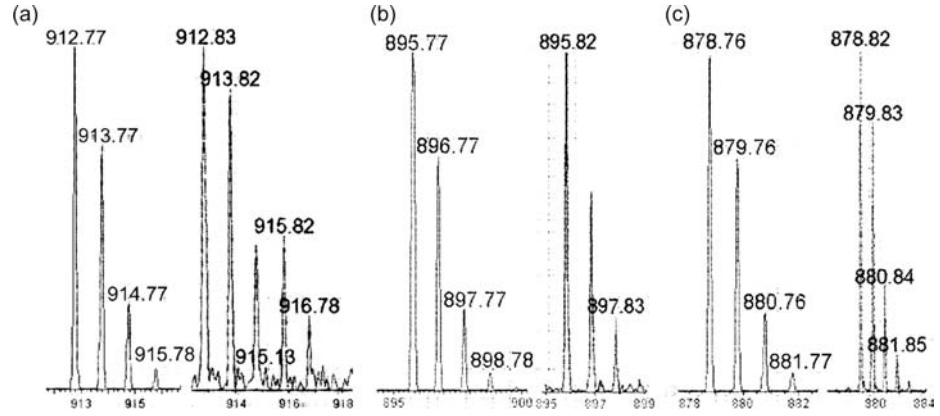

Figure 1. The MALDI TOF-MS of **OPVOH**. (a) The signals at *m/z* 912.83 correspond to M^+ (right). (b) The signals at *m/z* 894.82 correspond to $[M - OH^-]^+$ (right). (c) The signals at *m/z* 878.82 correspond to $[M - 2OH^-]^+$ (right). Calculated isotopic distributions (left).

Table 1. Gelation properties of **OPVBr** and **OPVOH** in various solvents.

Solvent	**OPVBr**	**OPVOH**	Solvent	**OPVBr**	**OPVOH**
n-Butanol	PG	S	Acetone	PS	PS
n-Octanol	G(35)[a]	PG	Toluene	PS	PS
Acetonitrile	PG	G(5)[a]	THF	PS	PS
n-Hexane	I	I	DMF	S	S
Nitrobenzene	PG	G(30)[a]	DMSO	S	S

Note: G, gel; S, soluble; I, insoluble; PS, poor solubility; PG, partial gelation.
[a]The CGC mg ml^{-1}.

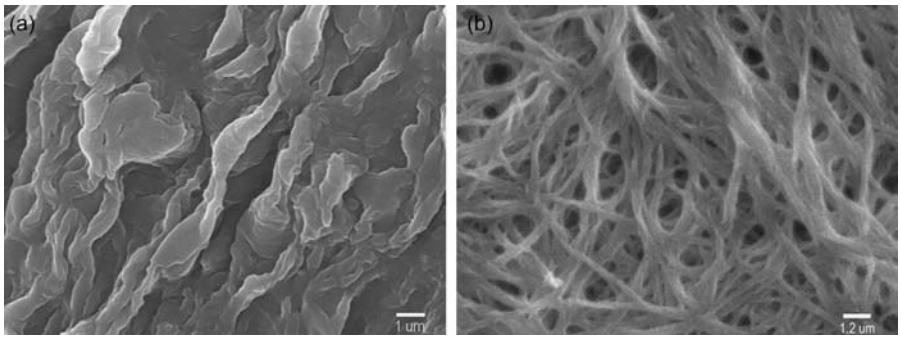

Figure 2. SEM images of xerogel (a) **OPVBr** from *n*-octanol and (b) **OPVOH** from acetonitrile.

OPVOH, the same effects were observed. As commonly observed in aromatic systems, the protons of one molecule in the aggregate are localized in the secondary magnetic field of the neighbouring aromatics, which results in a shielding effect depending on the size of the aggregates. Because the size of the aggregates in solution decreases at lower concentrations, a deshielding effect is observed in the concentration-dependent ^{1}H NMR spectra (*30*). Thus, the ^{1}H NMR chemical shift of the aromatic protons as the concentration changes implies that cation–π stacking between the gelator exists in the solution. We found that the change degrees in aromatic proton signals of **OPVBr** and **OPVOH** are different. This indicated that different counter-anions could cause different aggregate degrees in solution or different electron densities in the aromatic ring.

Figure 5 shows the temperature-dependent ^{1}H NMR spectra of **OPVOH** in *d*-acetonitrile recorded from 20 to 70°C. Upon increasing the temperature to 70°C, the gel gradually transformed into a solution with a downfield shift of the aromatic protons and N–CH_2 protons signals being observed. This result clearly indicated that the cation–π driving force assists 1D self-assembly of the gelator molecules and becomes stronger as the temperature decreases.

It is obvious that the gelation ability of **OPVBr** is relatively poor than that of **OPVOH**. In order to clarify the reason, FT-IR spectroscopy of **OPVOH** in chloroform solution and gel in acetonitrile was measured, as shown in Figure 6. There was a broad stretch vibration bond at 3446 and 3406 cm^{-1} in solution and gel, respectively, which indicated the presence of hydrogen bond. The remarkable low-frequency shift implies the stronger hydrogen bonding in gel. Therefore, the possible reason for better gelation ability of **OPVOH**, revealed by FT-IR spectroscopy, was that the counter-anion of pyridinium OH^- involved in hydrogen bonding made a directional effect. Thus, the aggregation morphology of **OPVOH** possesses higher regularity than that of **OPVBr**. Furthermore, there are some differences observed between solution and gel infrared absorption at the range of the stretching vibration of C=C (1650–1450 cm^{-1}) and bending vibration of aromatic protons (1000–400 cm^{-1}), which also provided the information about the existence of cation–π

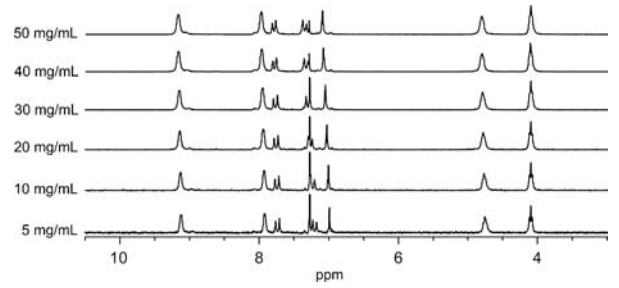

Figure 3. Concentration-dependent ^{1}H NMR spectra of **OPVBr** in $CDCl_3$ (5–50 mg ml^{-1}).

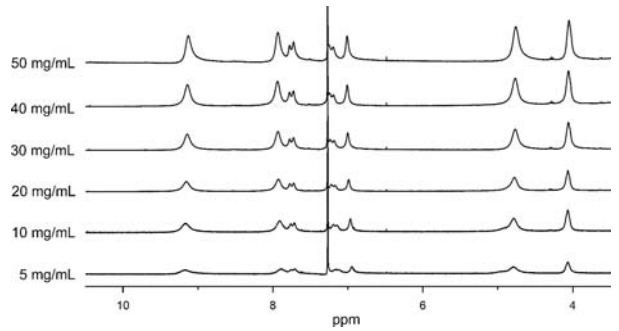

Figure 4. Concentration-dependent ^{1}H NMR spectra of **OPVOH** in $CDCl_3$ (5–50 mg ml^{-1}).

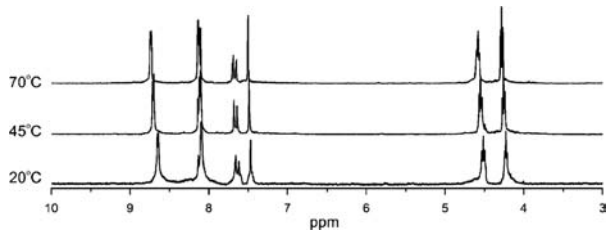

Figure 5. Temperature-dependent ^{1}H NMR spectra of **OPVOH** (10 mg ml^{-1}).

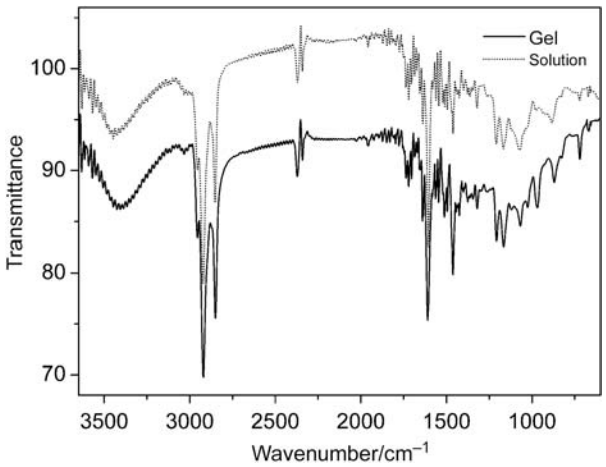

Figure 6. The FT-IR spectra of **OPVOH** in solution and gel.

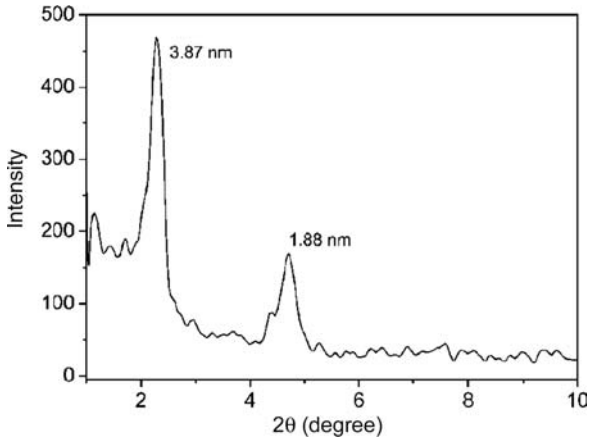

Figure 8. XRD pattern of a cast film from acetonitrile gel of **OPVOH**.

interaction between aromatic rings. The result agreed with the ^{1}H NMR measurement.

Time-dependent fluorescence spectral measurements were employed to monitor the supramolecular assembly process. As shown in Figure 7, the fluorescence spectrum of a hot **OPVOH** solution (5 mg/ml, 70°C) in acetonitrile showed a emission peak at 578 nm. Upon cooling the hot solution to room temperature, the emission peak red shifted to 600 nm, whereas the emission intensity decreased gradually. This result indicated that the aggregation of **OPVOH** in gel is likely to be in the form of a *J*-type mode (*31*).

The XRD patterns of **OPVOH** xerogel from acetonitrile were recorded and are shown in Figure 8. The xerogel exhibited two sets of diffraction peaks: $2\theta = 2.28°$ and 4.70° corresponding to $d = 3.87$ and 1.88 nm in the ratio of 1:0.5. The ratios of these d values suggest the existence of a lamellar organisation in the gel state. On the basis of XRD, Fl and molecular calculation, the possible self-assembling mode for the organogel **OPVOH** can be illustrated as shown in Figure 9. As demonstrated, the gelators could pack into 1D molecular fibre units in a typical face-to-face manner through the driving forces of cation–π, van der Waals interactions and hydrogen bonding interactions between OH^-. In the lamellar packing, **OPVOH** adopts a planar structure, in which the aryl units are coplanar and the *N*-alkyl chains are longitudinally extended, with a complete stretching of *N*-alkyl chains within the same plane as the conjugated back.

Owing to the presence of H-bond, the **OPVOH** gel could be disrupted by the addition of acid. As shown in Figure 10, there was an obvious modality change from gel to solution after adding of a drop of trifluoroacetic (TFA) acid. Meanwhile, its emission peak blue shifted and the fluorescence intensity increased significantly. The proposed reason for these phenomena was that TFA addition broke the hydrogen bonding between OH^- and at the same time the counter-anions were changed to fluoroacetate anion. Adding other acids such as HF and H_2SO_4, some effects could be obtained. When HBr was added, the gel modality was not disrupted, only a slight colour changed. But after another process of heating and cooling, the gel cannot be obtained. These results manifested that hydrogen bonding play an important role in the formation of self-

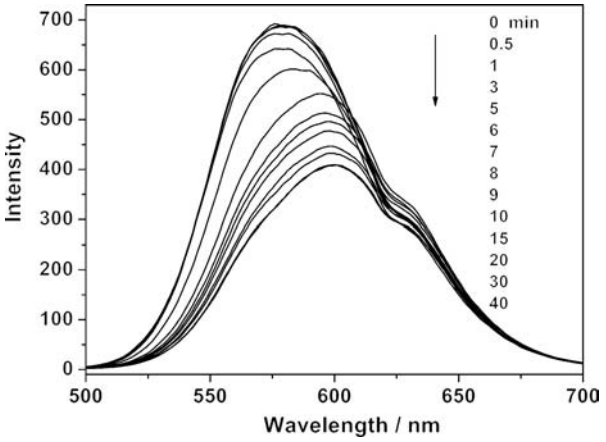

Figure 7. Time-dependent fluorescence spectra of a hot **OPVOH** solution in acetonitrile.

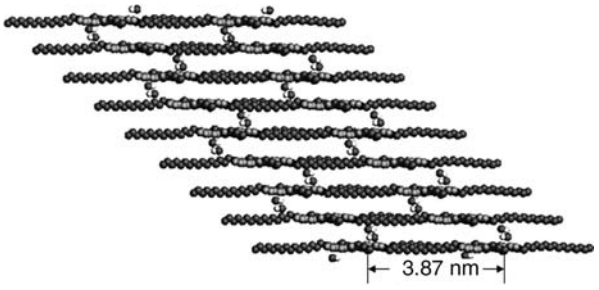

Figure 9. The possible molecular self-assembling packing mode for the organogel **OPVOH**.

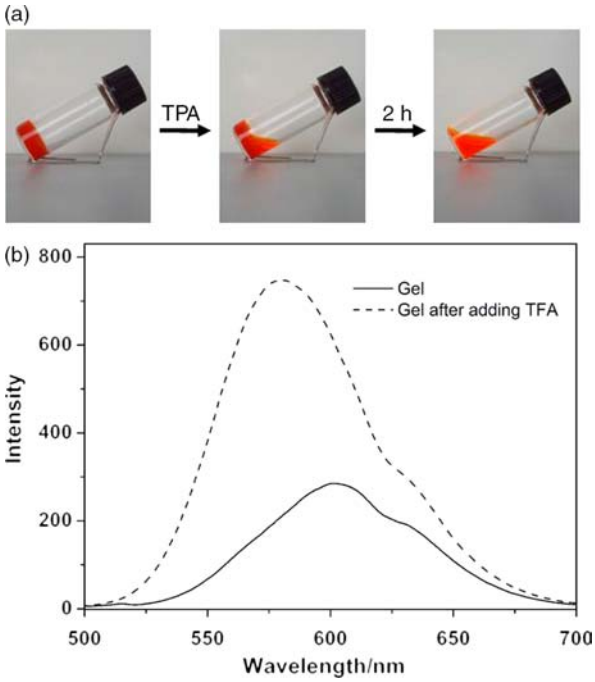

Figure 10. (a) Pictures of acetonitrile gel of **OPVOH** and after adding one drop of TFA on acetonitrile gel of **OPVOH**. (b) Fluorescence spectra of acetonitrile gel of **OPVOH** before and after adding one drop of TFA.

assembled structure, and the nature of the counter-anions has considerable influence on the gelation behaviour.

Interestingly, the xerogel of **OPVOH** also showed dramatic response to TFA (Figure 11). After exposing the xerogel to the vapour of TFA within a few seconds, significant fluorescence spectra change was observed. The fluorescence emission peak blue shifted from 637 to 581 nm, and the fluorescence intensity increased with the prolonging exposing time. These phenomena imply that the order of *J*-type aggregation of **OPVOH** was destroyed by TFA. It is interesting to note that when the xerogel stood 20 min in air after TFA exposure, the fluorescence spectra were almost restored. Then the xerogel was exposed to the vapour of TFA once more, and the same change of fluorescence spectra like the first time could be observed. These results indicated that the xerogel of **OPVOH** could be a potential acid sensor.

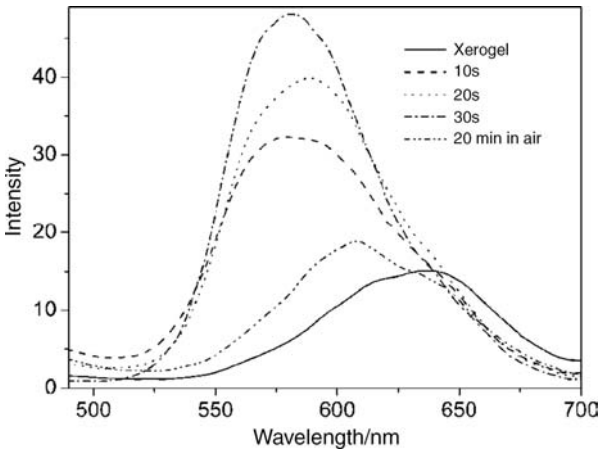

Figure 11. Fluorescence spectra of **OPVOH** xerogel before and after exposure to the vapour of TFA.

Conclusion

In summary, two stilbazolium derivative gelators with different counter-anions Br^- and OH^- were successfully synthesised. Their gelation property studies revealed that the gelation ability of **OPVOH** is much better than that of **OPVBr**. This difference is mainly attributed to the hydrogen bonding between OH^- in **OPVOH** gelation process. The gel of **OPVOH** in acetonitrile could be disrupted by the addition of acid and the xerogel film of **OPVOH** exhibited a good acid-sensing abilitiy.

Experimental part

Materials and instruments

All chemicals were purchased from Aldrich (Beijing, China) and used as received without further purification. For chromatography, 100–200 mesh silica gel (Qingdao, China) was employed. Fluorescence spectra were determined on a fluorescence spectrophotometer (RF-540). NMR spectra were recorded on a Bruker AV-300 spectrometer. Chemical shifts are reported in ppm using tetramethylsilane as the internal standard. The mass spectra were performed on a Shimadzu MALDI AXIMA-CFR$^+$ spectrometer. The SEM images were examined by scanning electron microscopy (Hitachi S-3500N).

Synthesis

2,5-Di-(*n*-butoxy)terephthalaldehyde was synthesised according to the literature (*27*).

4,4′-(1E,1′E)-2,2′-(2,5-dibutoxy-1,4-phenylene)bis(ethene-2,1-diyl)bis(1-hexadecylpyridinium) bromide (OPVBr)

To an ethanol solution of 2,5-di-(*n*-butoxy)terephthalaldehyde (1 eq.) and 1-hexadecyl-4-methylpyridinium bromide (2 eq.) was added piperidine (2 eq.) at room temperature. The mixture was continuously stirred and refluxed for 24 h. After cooling down, the red precipitate was filtrated, and the residue was then recrystallised two times using acetonitrile. Yield: 76%. ^{1}H NMR (300 MHz, $CDCl_3$) δ: 9.11 (d, $J = 5.7$ Hz, 4H), 7.91 (d, $J = 5.7$ Hz, 4H), 7.74 (d, $J = 16.4$ Hz, 2H), 7.19 (d, $J = 16.4$ Hz, 2H), 6.98 (s, 2H), 4.75 (t, $J = 5.4$ Hz, 4H), 4.09 (t, $J = 5.4$ Hz, 4H), 1.96–1.92 (m, 8H), 1.66–1.59 (m, 4H), 1.33–1.29

(m, 8H), 1.27–1.21 (m, 44H), 1.09 (t, $J = 7.3$ Hz, 6H), 0.88 (t, $J = 6.8$ Hz, 6H). ^{13}C NMR (75 MHz, $CDCl_3$) δ: 153.17, 152.12, 144.40, 135.45, 126.61, 123.98, 123.74, 111.73, 69.04, 60.74, 32.41, 31.88, 31.80, 31.39, 29.65, 29.48, 29.33, 29.09, 27.94, 26.08, 22.65, 19.50, 14.43. MALDI TOF-MS, $[M - Br]^+$: 957.73, $[M - 2Br]^+$: 878.78.

4,4′-(1E,1′E)-2,2′-(2,5-dibutoxy-1,4-phenylene)bis(ethene-2,1-diyl)bis(1-hexadecylpyridinium) hydroxide (OPVOH)

Anion exchange resin was used as column chromatography filler, which was treated by NaOH solution, and then washed by water to neutral. **OPVOH** was obtained by treating **OPVBr** solution with anion exchange resin column. ^{1}H NMR (300 MHz, $CDCl_3$) δ: 9.17 (s, 4H), 7.91 (s, 4H), 7.76 (d, $J = 16.1$ Hz, 2H), 7.19 (d, $J = 16.1$ Hz, 2H), 6.99 (s, 2H), 4.80 (s, 4H), 4.07 (s, 4H), 1.96–1.92 (m, 8H), 1.66–1.59 (m, 4H), 1.33–1.29 (m, 8H), 1.27–1.21 (m, 44H), 1.08 (t, $J = 7.3$ Hz, 6H), 0.87 (t, $J = 6.8$ Hz, 6H). ^{1}H NMR (300 MHz, MeOH) δ: 8.82 (d, $J = 6.5$ Hz, 4H), 8.16 (d, $J = 16.2$ Hz, 2H), 8.15 (d, $J = 6.5$ Hz, 4H), 7.66 (d, $J = 16.2$ Hz, 2H), 7.47 (s, 2H), 4.55 (t, $J = 7.4$ Hz, 4H), 4.21 (t, $J = 6.4$ Hz, 4H), 2.04–2.01 (m, 4H), 1.97–1.88 (m, 4H), 1.68–1.58 (m, 4H), 1.42–1.38 (m, 8H), 1.38–1.16 (m, 44H), 1.06 (t, $J = 7.4$ Hz, 6H), 0.89 (t, $J = 6.8$ Hz, 6H). ^{13}C NMR (75 MHz, MeOH) δ: 154.18, 152.36, 143.91, 135.64, 127.12, 124.49, 123.87, 111.87, 68.85, 60.54, 31.66, 31.08, 30.89, 29.38, 29.07, 28.66, 25.72, 22.33, 19.14, 12.99, 12.85. MALDI TOF-MS, $[M - OH]^+$: 992.75, $[M - 2OH]^+$: 878.76.

Acknowledgement

We gratefully acknowledge financial support from the Ph.D. Programmes Foundation of Ministry of Education of China (No. 20092201110001).

References

(1) Sugiyasu, K.; Fujita, N.; Shinkai, S. *J. Mater. Chem.* **2005**, *15*, 2747–2754.
(2) Lee, D.-C.; McGrath, K.K.; Jang, K. *Chem. Commun.* **2008**, 3636–3638.
(3) Nakayama, D.; Takeoka, Y.; Watanabe, M.; Kataoka, K. *Angew. Chem. Int. Ed.* **2003**, *42*, 4197–4201.
(4) Seo, S.H.; Chang, J.Y. *Chem. Mater.* **2005**, *17*, 3249–3254.
(5) Brignell, S.V.; Smith, D.K. *New J. Chem.* **2007**, *31*, 1243–1249.
(6) Xue, P.; Lu, R.; Li, D.; Jin, M.; Bao, C.; Zhao, Y.; Wang, Z. *Chem. Mater.* **2004**, *16*, 3702–3707.
(7) Huang, X.; Weiss, R.G. *Langmuir* **2006**, *22*, 8542–8552.
(8) Kawano, S.-I.; Tamaru, S.-I.; Fujita, N.; Shinkai, S. *Chem. Eur. J.* **2004**, *10*, 343–351.
(9) Xia, Y.; Wang, Y.; Chen, K.; Tang, L. *Chem. Commun.* **2008**, 5113–5115.
(10) Terech, P.; Weiss, R.G. *Chem. Rev.* **1997**, *97*, 3133–3159.
(11) Ajayaghosh, A.; Praveen, V.K. *Acc. Chem. Res.* **2007**, *40*, 644–656.
(12) Sangeetha, N.M.; Maitra, U. *Chem. Soc. Rev.* **2005**, *34*, 821–836.
(13) Brunsveld, L.; Folmer, B.J.B.; Meijer, E.W.; Sijbesma, R.P. *Chem. Rev.* **2001**, *101*, 4071–4097.
(14) Yamada, S. *Org. Biomol. Chem.* **2007**, *5*, 2903–2912.
(15) Hunter, C.A.; Lawson, K.R.; Perkins, J.; Urch, C.J. *J. Chem. Soc. Perkin Trans.* **2001**, *2*, 651–669.
(16) Nishio, M.; Umezawa, Y.; Hirota, M.; Takeuchi, Y. *Tetrahedron* **1995**, *51*, 8665–8701.
(17) Gokel, G.W.; Barbour, L.J.; Ferdani, R.; Hu, J. *Acc. Chem. Res.* **2002**, *35*, 878–886.
(18) Meyer, E.A.; Castellano, R.K.; Diederich, F. *Angew. Chem., Int. Ed.* **2003**, *42*, 1210–1250.
(19) Tu, T.; Assenmacher, W.; Peterlik, H.; Schnakenburg, G.; Dötz, K.H. *Angew. Chem. Int. Ed.* **2008**, *47*, 7127–7131.
(20) Xiao, S.; Zou, Y.; Yu, M.; Yi, T.; Zhou, Y.; Li, F.; Huang, C. *Chem. Commun.* **2007**, 4758–4760.
(21) George, S.J.; Ajayaghosh, A. *Chem. Eur. J.* **2005**, *11*, 3217–3227.
(22) Srinivasan, S.; Babu, S.S.; Praveen, V.K.; Ajayaghosh, A. *Angew. Chem. Int. Ed.* **2008**, *47*, 5746–5749.
(23) Ajayaghosh, A.; Praveen, V.K.; Srinivasan, S.; Varghese, R. *Adv. Mater.* **2007**, *19*, 411–415.
(24) Babu, S.S.; Praveen, V.K.; Prasanthkumar, S.; Ajayaghosh, A. *Chem. Eur. J.* **2008**, *14*, 9577–9584.
(25) Babu, S.S.; Kartha, K.K.; Ajayaghosh, A. *J. Phys. Chem. Lett.* **2010**, *1*, 3413–3424.
(26) Tong, X.; Zhao, Y.; An, B.-K.; Park, S.Y. *Adv. Funct. Mater.* **2006**, *16*, 1799–1804.
(27) Srinivasan, S.; Babu, P.A.; Mahesh, S.; Ajayaghosh, A. *J. Am. Chem. Soc.* **2009**, *131*, 15122–15123.
(28) Vijayakumar, C.; Praveen, V.K.; Ajayaghosh, A. *Adv. Mater.* **2009**, *21*, 2059–2063.
(29) Zhu, G.Y.; Dordick, J.S. *Chem. Mater.* **2006**, *18*, 5988–5995.
(30) Wu, J.S.; Fechtenkötter, A.; Gauss, J.; Watson, M.D.; Kastler, M.; Fechtenkötter, C.; Wagner, M.; Müllen, K. *J. Am. Chem. Soc.* **2004**, *126*, 11311–11321.
(31) Peng, A.-D.; Xiao, D.-B.; Ma, Y.; Yang, W.-S.; Yao, J.-N. *Adv. Mater.* **2005**, *17*, 2070–2073.